2010 IEEE International Conference on Robotics and Automation
Anchorage Convention District
May 3-8, 2010, Anchorage, Alaska, USA

Optimal Ball Pitching with an Underactuated Model of a Human Arm

Uwe Mettin, Anton S. Shiriaev, Leonid B. Freidovich, Mitsuji Sampei

***Abstract*— A new approach for solving an optimal control problem of ball pitching with an underactuated human-like robot arm is proposed. The system dynamics is simplified to a planar two-link robot with actuation only at the shoulder joint and a passive spring at the elbow joint representing the stiffness of the arm. The objective is to accelerate the ball from an initial configuration at rest in such a way that the projection of its velocity along a certain elevation angle is maximal at a predefined release line. The suggested procedure makes use of a parameterization of the robot motion in terms of geometric relations among the generalized coordinates. We systematically formulate a necessary condition for an optimal motion resulting in a nonlinear differential equation that describes a synchronization of the joint angles. A suitable solution is found by numerically searching over a finite number of free initial conditions.**

***Index Terms*— Underactuated Mechanical Systems, Optimal Control, Motion Planning**

I. Introduction

How do humans pitch a ball or throw a javelin? What is the motor control pattern associated with the motion? How to train an athlete in order to optimize the trajectory? These are interesting questions in research fields ranging from medical science to robotics and control engineering.

In order to approach these questions we suggest an analytical procedure for a simple but still representative model that describes the dynamical interaction of the main parts of the human body involved in the pitching motion. The model of a two-link pendulum is used with actuation at the shoulder and a passive spring-loaded elbow joint accounting for the arm stiffness. We search a motion for which the ball attached to the end effector reaches the maximal velocity along a certain elevation angle at a predefined release line when started from a resting position. Although we do not constrain the magnitude of the controlled torque at the shoulder, the lack of direct actuation at the second joint[1] limits reachable ball velocities at the release line. Note that it is not a problem to deal with more complex models that have additional actuated degrees of freedom.

U. Mettin, L. Freidovich, and A. Shiriaev are with the Department of Applied Physics and Electronics, Umeå University, SE-901 87 Umeå, Sweden. E-mail: Uwe.Mettin@tfe.umu.se.

U. Mettin and A. Shiriaev are also with the Department of Engineering Cybernetics, Norwegian University of Science and Technology, NO-7491 Trondheim, Norway.

M. Sampei is with the Department of Mechanical and Control Engineering, Tokyo Institute of Technology, 2-12-1 Oh-Okayama Meguro-ku Tokyo, Japan.

This work has been partly supported by the Kempe Foundation and the Swedish Research Council (under grants 2005-4182 and 2008-4369).

[1] A linear spring added at the second joint can generate only certain torque profiles and is considered as a part of the dynamical model rather than an actuator.

The main contribution of this paper is a particular characterization of a class of optimal motions for mechanical systems with underactuation degree one. We show that, if such an optimal motion exists, then by necessity there is a geometric function among the generalized coordinates that can be found as a solution of a particular nonlinear differential equation with coefficients determined by the physical parameters of the robot. For certain initial conditions, which are partly given by the initial configuration and initial control torque, it is possible to reconstruct an (at least locally) optimal trajectory.

The interest in human-like ball pitching robots reaches back to a patent [8] in the 1960's. Nowadays there is a large number of experimental setups for studying human-like ball-pitching motions and numerous videos and news can be easily found in the internet. For a 2-degrees-of-freedom model, such as introduced above, we can find some control strategies reported in [3], [4], [6]. Detailed analysis of the throwing system, physical characteristics, and performance of a control strategy in experiments are presented in [4], where a model with constraints instead of a spring is analyzed as well. A deceleration control strategy is proposed in [6] based on analysis of zero dynamics.

In this paper we concentrate on the motion planning procedure for optimal ball pitching. The problem statement and some preliminaries are discussed in Section II. In Section III we present the main result: a necessary condition valid along an optimal pitching motion, provided it exists. It is written in the form of an integral-differential dynamical system, which is satisfied by a function that represents a synchronization of the joint angles. A numerical study is presented in Section IV. A discussion of the results together with some concluding remarks are given in Section V. Experimental studies are intended for future work.

II. Preliminaries and Problem Formulation

A. Modeling the Arm Dynamics

Approximating the dynamics of a human arm in general by the that of a two-link planar pendulum clearly oversimplifies the description of the system. Indeed, several degrees of freedom together with the 3D nature of the trajectory are neglected, spin effects through fingers and wrist, internal dynamics in muscles as well as sensory and feedback mechanisms in grasping are dropped. Meanwhile, it is apparent that for fast motions such as pitching, the dynamics of a two-link planar pendulum is relevant and captures the main parts of the dynamical behavior of the arm responsible for accelerating a ball in the hand.

978-1-4244-5040-4/10/$26.00 ©2010 IEEE

The equations of motion of the two-link planar pendulum with shoulder and elbow joints (see Fig. 1) are compactly written as

$$\frac{d}{dt}\left[\frac{\partial \mathcal{L}}{\partial \dot{q}_1}\right] - \frac{\partial \mathcal{L}}{\partial q_1} = \tau_{q_1}\,, \qquad \frac{d}{dt}\left[\frac{\partial \mathcal{L}}{\partial \dot{q}_2}\right] - \frac{\partial \mathcal{L}}{\partial q_2} = \tau_{q_2}\,, \quad (1)$$

where $\mathcal{L} = (K_1 + K_2 + K_b) - (\Pi_1 + \Pi_2 + \Pi_b)$ is the Lagrangian formed by the kinetic and potential energies of the 1st and 2nd links and the ball, respectively (see Appendix A for explicit expressions and model parameters). The signal τ_{q_1} is the generalized torque at the shoulder and should be presumably of large amplitude for moving the whole arm, while the signal τ_{q_2} is the generalized torque at the elbow and expected to be smaller.

Bio-mechanical mechanisms for generating the torque τ_{q_2} in an elbow of a human arm as well as ways for approximating it are important points for a discussion. There are no doubts that an elbow is actively controlled during a human pitching motion. However, there are several reasons to postulate that for the model (1) the signal τ_{q_2} is mainly generated by an elastic element (see also [1]):

- The elbow moves quickly with high amplitude, which can be interpreted as well-tuned open loop control strategy that can be realized by a spring-like actuator.
- Passive or semi-passive actuation at the elbow joint does not necessarily restrict possible motions, but rather allows to have reasonable and human-like proportions of mass distribution, torque levels and response time.
- If the second link would be directly actuated, then the search for an optimal pitching trajectory should take into account the limits of τ_{q_2}. Otherwise an optimal motion does not exist, since the arm could move as fast as possible even within an arbitrary short interval of time. Assuming that the second link is not actuated but spring-loaded, we can remove such limitation and search for a motion that utilizes dynamical properties of the mechanical structure as much as possible.

From now it will be assumed that the torque τ_{q_2} is generated by a linear spring[2]

$$\tau_{q_2} = -K\left(q_2 - q_1 - q_{\text{off}}\right)\,, \quad (2)$$

where the spring coefficient K and the offset q_{off} are constants. Combining the second equation of (1) with (2), we obtain the equation of motion for the second link as

$$\frac{d}{dt}\left[\frac{\partial \mathcal{L}}{\partial \dot{q}_2}\right] - \frac{\partial \mathcal{L}}{\partial q_2} + K\left(q_2 - q_1 - q_{\text{off}}\right) = 0\,. \quad (3)$$

It has no control input, so the mechanical system (1) is underactuated with one passive link; this type of two-link pendulum is also known as Pendubot [7], but here equipped with a spring about the elbow joint.

[2]All arguments below can be repeated in the same way if the spring has a non-linear characteristic.

B. Problem Formulation

An initial configuration of the two-link pendulum (1)–(2) at $t = 0$ is given (see Fig. 1(a)). Let the vertical line $x = X_b(R)$ be the pitching line at which the ball shall be released (see Fig. 1(b)). The problem is to *determine the optimal trajectory of the ball, i.e. finding*

- *time evolution of the generalized coordinates* $q_1(t)$ *and* $q_2(t)$*,*
- *time evolution of the external (control) torque* $\tau_{q_1}(t)$*,*
- *the duration of the motion* $T_R > 0$*,*

such that the horizontal component of the final ball velocity $V_{bx}(T_R)$ *is maximized at the release line* $x = X_b(R)$ *starting from rest at* $x = X_b(B)$. Here we assume that the end effector can be adjusted to a desired elevation angle at ball release. One could also choose to maximize the final ball velocity along an angle different from the horizontal. The considerations shall be restriced to smooth pitching motions only.

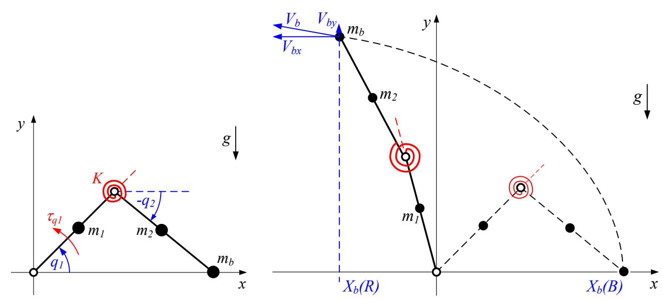

(a) The initial configuration of the two-link pendulum.

(b) The final configuration and target trajectory.

Fig. 1. The problem is to determine the trajectory of the ball and the corresponding behavior of both links starting at rest at the initial configuration and ending at the release point with maximum ball velocity in the horizontal direction.

III. Main Result: Characterization of Optimal Pitching for the System (1)–(2)

Let us assume that the optimal pitching trajectory

$$q_1 = q_{1\star}(t), \quad q_2 = q_{2\star}(t), \quad t \in [0, T_R] \quad (4)$$

from a given configuration $[q_{1\star}(0), q_{2\star}(0)]$ indeed exists.

Below we suggest a series of steps to convert the stated problem into a problem of finding initial conditions for a nonlinear differential equation.

Step 1

Let us note that for an optimal trajectory (4) we must have an optimal evolution of the abscissa of the ball coordinates in the inertia frame defined as (see Fig. 1):

$$X_{b\star}(t) = l_1 \cos(q_{1\star}(t)) + l_2 \cos(q_{2\star}(t))$$

evolving from $X_{b\star}(0) = X_b(B)$ to $X_{b\star}(T_R) = X_b(R)$.

Since the optimization problem is formulated in terms of the abscissa of the ball coordinates, it makes sense to reformulate our dynamics accordingly. Suppose that the implicit parameterization of the optimal motion by a scalar variable t is resolved on some sub-interval[3] of the interval $[0, T_R]$ and the geometric function $\phi_\star(X_b)$ is found as

$$q_{1\star}(t) = \phi_\star\left(X_{b\star}(t)\right) , \tag{5}$$

then we must have

$$q_{2\star}(t) = \arccos\left(\frac{X_{b\star}(t) - l_1\cos(\phi_\star\left(X_{b\star}(t)\right))}{l_2}\right) . \tag{6}$$

The task of finding $q_{1\star}(t)$ and $q_{2\star}(t)$ can be reformulated as the problem of finding $X_{b\star}(t)$ and $\phi_\star(X_b)$ by introducing the change of coordinates

$$q_1 = \phi\left(X_b\right), \quad q_2 = \arccos\left(\frac{X_b - l_1\cos(\phi\left(X_b\right))}{l_2}\right) . \tag{7}$$

Step 2

Rewriting the non-actuated equation (3) in the new coordinates (7) gives the following scalar 2nd-order differential equation

$$\alpha\left(X_b, \phi, \phi'\right)\ddot{X}_b(t) + \beta\left(X_b, \phi, \phi', \phi''\right)\dot{X}_b^2(t) + \gamma\left(X_b, \phi\right) = 0 , \tag{8}$$

which describes the time evolution of the independent configuration variable X_b, given a C^2–smooth function $\phi(X_b)$. Explicit expression of the scalar coefficient functions $\alpha(\cdot)$, $\beta(\cdot)$, and $\gamma(\cdot)$ can be found in Appendix B.

Note also that solutions of (8) together with the new coordinates (7) can be used to compute the control torque τ_{q1} in the first equation of the system dynamics (1) along a particular trajectory.

Step 3

The equation (8) is integrable in closed form [5]. Straightforward calculations show that the value of the function

$$\begin{aligned} & I\left(X_b(0), \dot{X}_b(0), X_b(t), \dot{X}_b(t)\right) = \\ & = \dot{X}_b^2(t) - \exp\left\{-2\int_{X_b(0)}^{X_b(t)} \frac{\beta\left(\tau,\phi(\tau),\phi'(\tau),\phi''(\tau)\right)}{\alpha\left(\tau,\phi(\tau),\phi'(\tau)\right)}d\tau\right\}\dot{X}_b^2(0) \\ & + \int_{X_b(0)}^{X_b(t)} \exp\left\{2\int_{X_b(t)}^{s} \frac{\beta\left(\tau,\phi(\tau),\phi'(\tau),\phi''(\tau)\right)}{\alpha\left(\tau,\phi(\tau),\phi'(\tau)\right)}d\tau\right\} \frac{2\gamma\left(s,\phi(s)\right)}{\alpha\left(s,\phi(s),\phi'(s)\right)}ds \end{aligned} \tag{9}$$

is kept *zero* for all $t \geq 0$ along any well-defined solution of the system (8).

By assumption, the two-link pendulum (1) is at rest in the beginning of the motion. Therefore, the desired ball velocity $\dot{X}_{b\star}(0)$ is zero even though the acceleration $\ddot{X}_{b\star}(0)$ might be different from zero due to external torques. With such initial conditions we can exploit the conserved quantity (9) as determining equation for the velocity at the end of the pitching motion, i.e. for $t = T_R$ it follows:

$$\begin{aligned} & \dot{X}_b^2(T_R) = \\ & \int_{X_b(0)}^{X_b(R)} -\exp\left\{2\int_{X_b(R)}^{s} \frac{\beta\left(\tau,\phi(\tau),\phi'(\tau),\phi''(\tau)\right)}{\alpha\left(\tau,\phi(\tau),\phi'(\tau)\right)}d\tau\right\} \frac{2\gamma\left(s,\phi(s)\right)}{\alpha\left(s,\phi(s),\phi'(s)\right)}ds \end{aligned} \tag{10}$$

[3] Actually, one needs to partition the time interval $[0, T_R]$ into singularity-free sub-intervals. The arguments below should be applied to each sub-interval of such a partition. However, below we will show the result for only one of them.

For the optimal motion (5) the value of $\dot{X}_b(t)$ at $t = T_R$ is maximal. Therefore, the function $\phi_\star(\cdot)$ defined by (5) is not arbitrary, but the maximizer for the performance index

$$\begin{aligned} J = \int_{X_b(0)}^{X_b(R)} -\exp\left\{2\int_{X_b(R)}^{s} \frac{\beta\left(\tau,\phi(\tau),\phi'(\tau),\phi''(\tau)\right)}{\alpha\left(\tau,\phi(\tau),\phi'(\tau)\right)}d\tau\right\} \\ \times \frac{2\gamma\left(s,\phi(s)\right)}{\alpha\left(s,\phi(s),\phi'(s)\right)}ds \to \max . \end{aligned} \tag{11}$$

Step 4

The functions $\alpha(\cdot)$ and $\beta(\cdot)$ in the performance index (11) have the following structure

$$\begin{aligned} \alpha\left(\tau, \phi, \phi'\right) &= \rho_1\left(\tau, \phi\right)\cdot\phi' + \rho_2\left(\tau, \phi\right) \\ \beta\left(\tau, \phi, \phi', \phi''\right) &= \rho_1\left(\tau, \phi\right)\cdot\phi'' + \rho_3\left(\tau, \phi, \phi'\right) , \end{aligned} \tag{12}$$

where $\rho_1(\cdot)$, $\rho_2(\cdot)$, $\rho_3(\cdot)$ can be obtained from the expressions of $\alpha(\cdot)$ and $\beta(\cdot)$ used in (8). We can exploit this structure for rewriting the first factor in (11) independent of $\phi''(\cdot)$ such that the optimization task takes the standard form[4]

$$\int_{X_b(0)}^{X_b(R)} \Psi\left(s, \phi(s), \phi'(s)\right)ds \to \max \tag{13}$$

with

$$\begin{aligned} \Psi = -\exp\left\{2\int_{X_b(R)}^{s} \frac{\rho_3\left(\tau,\phi,\phi'\right) - \rho_1'\left(\tau,\phi\right)\phi' - \rho_2'(\tau,\phi)}{\rho_1(\tau,\phi)\phi' + \rho_2(\tau,\phi)}d\tau\right\} \\ \times \left[\frac{\rho_1(s,\phi)\cdot\phi' + \rho_2(s,\phi)}{\rho_1(X_b(0),\phi)\cdot\phi' + \rho_2(X_b(0),\phi)}\right]^2 \frac{2\gamma(s,\phi)}{\alpha(s,\phi,\phi')} . \end{aligned} \tag{14}$$

It is a well-known fact [2] that, if a maximizer $\phi(\cdot)$ of (13) is C^2–smooth, then by necessity it should satisfy the Euler–Lagrange equation

$$\frac{d}{ds}\left[\frac{\partial}{\partial\phi'}\Psi\right] - \frac{\partial}{\partial\phi}\Psi = 0 . \tag{15}$$

This is not a differential equation with respect to time, it is written in terms of a variable that parameterizes the position on the trajectory of an optimal motion. In fact, it is an integral-differential equation that can be equivalently rewritten[5] as a 4th-order nonlinear differential equation with $\phi = \phi_\star(s)$ being a solution.

Summary

Let us summarize our findings.

Theorem 1: Consider the planar two-link pendulum (1) such that the external torque at the elbow joint is generated by a spring (2), whereas the torque at the shoulder joint is a variable that can be chosen arbitrary. Suppose that there exists a C^2–smooth optimal pitching motion for a given starting configuration of the robot (1), which is the solution of the problem stated in Section II. Then, by necessity, there exists the function $\phi_\star(s)$ defined by (5), which must be a solution of the equation (15). ■

[4] Detailed steps can be found in Appendix C.

[5] It can be done provided the solutions are smooth.

IV. Numerical Solution

In this section we present two out of many solutions of equation (15) computed numerically. The corresponding pitching trajectory of the robot (1)–(2) is finally obtained by solving the reduced dynamics (8). The physical model parameters of the two-link pendulum (1)–(2) used for the numerical study are given in Appendix A.

Considering only C^4–smooth solutions of the integral-differential equation (15) allows to rewrite it as the following 4th-order differential equation

$$\phi^{(4)}(X_b) = f\left(X_b, \phi(X_b), \phi'(X_b), \phi''(X_b), \phi^{(3)}(X_b)\right) \quad (16)$$

with respect to the independent variable X_b. Numerical integration of (16) requires the initial conditions

$$\left[x_0 = X_b(0),\, \phi(x_0),\, \phi'(x_0),\, \phi''(x_0),\, \phi^{(3)}(x_0)\right] . \quad (17)$$

The values for x_0 and $\phi(x_0)$ are given by the initial configuration of the robot

$$\begin{aligned} x_0 &= \left[X_b(t) = l_1 \cos q_1(t) + l_2 \cos q_2(t)\right]\Big|_{t=0} \\ \phi(x_0) &= \left[\phi(X_b(t)) = q_1(t)\right]\Big|_{t=0} . \end{aligned}$$

Providing a value for the initial control torque $\tau_{q_1}(0)$ makes it possible to find the initial value for $\phi'(x_0)$

$$\phi'(x_0) = h\left(x_0, \phi(x_0), \tau_{q_1}(0)\right)$$

using the expressions for the second derivatives $\ddot{q}(0)$ from (1)–(2) and $\ddot{X}_b(0)$ from (8). Note that the velocities $\dot{q}(0)$ and $\dot{X}_b(0)$ are all equal to zero given the fact that the motion starts from a resting position. The initial conditions $\phi''(x_0)$ and $\phi^{(3)}(x_0)$ can be obtained providing the values for $\dot{\tau}_{q_1}(0)$ and $\ddot{\tau}_{q_1}(0)$, which to some extent are free values to choose.

Let us consider the following initial configuration of the robot:

$$\left.\begin{aligned} q_1(0) &= \pi/2 - 0.15\,\text{rad} \\ q_2(0) &= q_1(0) - 0.5\,\text{rad} \end{aligned}\right\} \Rightarrow \left\{\begin{aligned} x_0 &= 0.35\,\text{m} \\ \phi(x_0) &= 1.421\,\text{rad}\,, \end{aligned}\right.$$

such that we can solve the differential equation (16) on the interval $X_b \in [-0.35, 0.35]$ without occurence of singularities[6], where the inital ball postion is $X_b(0) = 0.35\,\text{m}$ and $X_b(T_R) = -0.35\,\text{m}$ is the ball positon at the release line. Further, we choose an initial control torque $\tau_{q_1}(0) = 2\,\text{Nm}$ determining $\phi'(x_0)$ as depicted in Fig. 2(a). The effect of varying the initial conditions $\phi''(x_0)$ and $\phi^{(3)}(x_0)$ on the solution[7] of (16) is visualized in Fig. 2(b) in terms of the final ball velocity $\dot{X}_b(T_R)$ at the release line[8], which can be computed solving (9). Singularities occur for $\phi''(x_0) > 0$, which is the reason why the grid in Fig. 2(b) ends there; varying $\phi^{(3)}(x_0)$ is obviously insignificant to the solution.

Here we illustrate the two cases of possible initial conditions (17) shown in Fig. 2:

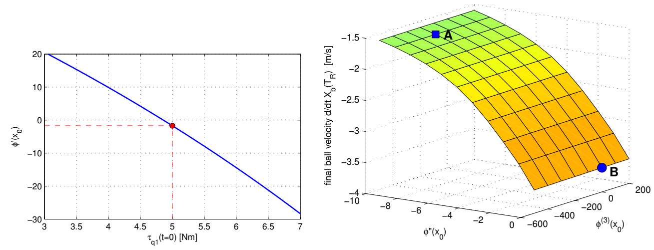

(a) Initial torque $\tau_{q_1}(0)$ determining $\phi'(x_0)$.

(b) Final ball velocity $\dot{X}_b(T_R)$ at the release line with respect to initial conditions $\phi''(x_0)$ and $\phi^{(3)}(x_0)$. The final ball velocity is negative.

Fig. 2. Choice for initial conditions of (16).

- **(A)** The magnitude of the final ball velocity is small, $\dot{X}_b(T_R) = -1.67\,\text{m/s}$: $\left[0.35,\, 1.421,\, -1.716,\, -9,\, -200\right]$.
- **(B)** The magnitude of the final ball velocity is about maximum, $\dot{X}_b(T_R) = -3.61\,\text{m/s}$: $\left[0.35,\, 1.421,\, -1.716,\, 0,\, 0\right]$.

The function $\phi(\cdot)$ that defines the geometric relation (5), obtained as solution of (16), is shown in Fig. 3 for initial conditions (**A**) and (**B**). Both curves have the same value for $X_b(0)$ but diverge significantly within the interval, which is a result of mainly varying the initial condition $\phi''(x_0)$. The

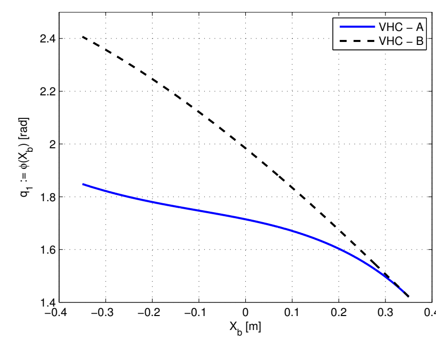

Fig. 3. Geometric relation (5) obtained as solution of the differential equation (16) for initial conditions (**A**) and (**B**), respectively.

corresponding pitching motion of the robot is schematically shown in Fig. 4. We can see that in case (**B**) the magnitude of the final velocity is much bigger compared with (**A**). The coordination pattern of the links looks also different, which is expected from Fig. 3.

The state space of X_b–dynamics (8) is depicted in Fig. 5(a) for the invariant geometric relations (5) found for cases (**A**) and (**B**), initialized at $[X_b(0),\, 0]$. Thus, the time evolution of X_b is automatically given, which, in fact, generates the motion of the robot through (5)–(6) within the interval $X_b \in [X_b(0),\, X_b(T_R)]$. Here we see that velocity profiles for the ball are different for different configuration patterns. In Fig. 5(b) we finally depict the nominal torque profiles $\tau_{q1}(q_1)$ of the actuated joint[9], which are required to

[6]Recall that the change of generalized coordinates (7) is local along the optimal motion (4), so singularities are likely to occur for (16).

[7]The solution is the function $\phi(\cdot)$ that defines the geometric relation (5).

[8]Note that the ball is accelerated against the direction of the x–coordinate, i.e. the final ball velocity is negative.

[9]Revisit Step 2 in Section III for details about computation of the control torque.

generate the individual pitching motions (**A**) and (**B**). In this representation one can also observe that the torque profile of case (**A**) could be generated by a passive spring.

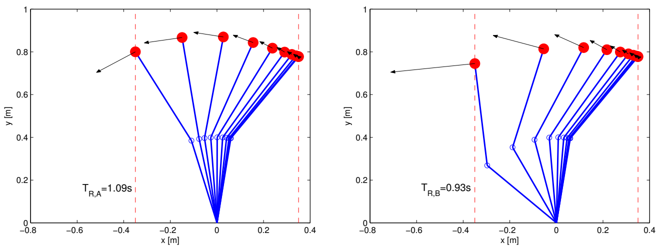

(a) Soluton for initial condition (**A**). The time span is $T_{R,A} = 1.09\,\mathrm{s}$.

(b) Soluton for initial condition (**B**). The time span is $T_{R,B} = 0.93\,\mathrm{s}$.

Fig. 4. Time instants of the robot configuration along the motion. The tangential velocity at the end of the second link is illustrated as arrow.

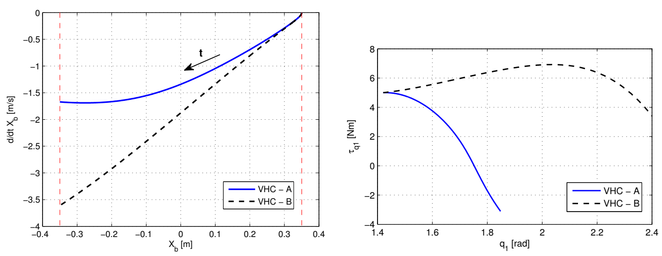

(a) Phase portrait of reduced dynamics (8). The final ball velocity is negative.

(b) Torque profile τ_{q1} of the actuated joint w.r.t. q_1 computed along the motion.

Fig. 5. Reduced dynamics and torque profile of the actuated joint found for the virtual holonomic constraint of the cases (**A**) and (**B**).

V. Discussion and Concluding Remarks

Let us comment the problem formulation and the content of Theorem 1:

1) It might be unusual that, instead of requesting to maximize the magnitude of the ball velocity at the release point along a particular direction, we search for the maximal projection onto a horizontal line. The reason for this is that the double pendulum can be always equipped with a wrist, which will allow to pitch a ball (or throw a javelin) along the prescribed direction such as athletes do. Solving both problems of maximizing the velocity and controlling the direction of the pitch appears to be too heavy for an underactuated robot.

2) Searching an optimal pitching motion for the underactuated mechanical system (1)–(2), as formulated in Section II, is a problem that requires a procedure for identifying a function of time: an external (control) torque $\tau_{q1}(t)$ defined for a finite but unknown time interval. This function must generate the optimal trajectory with maximal velocity at the end when started from a given robot configuration at rest.

Theorem 1 states another characterization of such a particular class of optimal motions. Instead of searching the optimal trajectory through computation of an external (control) signal $\tau_{q_1}(t)$, we converted the problem into a search of a finite vector of initial conditions (17) for the dynamical system (15) or (16) that describes a synchronization of the joint angles. Its solution satisfies the optimal pitching motion by necessity, provided it exists. As seen from the numerical study, at most two parameters are free for solving the problem: the first and second time derivatives of the external (control) torque at $t = 0$. However, due to possible singularities related to the parameterization of the optimal trajectory, it might be needed to partition the motion into sub-intervals. We have obtained an optimal solution for one of such intervals.

3) It is important to note that Theorem 1 is not limited to the studied two-link robot and can be generalized to mechanical systems with underactuation degree one.

4) Moreover, all the derivation steps would be almost identical for the case of a spring with a known nonlinear characteristic instead of a linear one.

5) Solving numerically the nonlinear equations (15) or (16) is a challenging task. However, the symbolic expressions have been obtained from straightforward computations using standard software.

6) The problem of maximizing the projection of the ball velocity onto another than horizontal line can be solved similarly. For example, if we are interested to pitch a ball (or throw a javelin) on the longest distance, then we should maximize the projection of the velocity along a certain elevation angle at a certain release point. The only difference in the derivations would be in parameterizing the motion in terms of this newly defined projection.

Appendix

A. Lagrangian and Equation of Motion

The Lagrangian $\mathcal{L} = (K_1+K_2+K_b)-(\Pi_1+\Pi_2+\Pi_b)$ of (1) is formed by the kinetic and potential energies of 1st and 2nd link and ball, respectively. Thus, the equation of motion for the planar two-link pendulum can be written as [7]:

$$M(q)\begin{bmatrix}\ddot{q}_1\\ \ddot{q}_2\end{bmatrix} + C(q,\dot{q})\begin{bmatrix}\dot{q}_1\\ \dot{q}_2\end{bmatrix} + G(q) = \begin{bmatrix}\tau_{q_1}\\ \tau_{q_2}\end{bmatrix},$$

where $G(q) = \left[p_4\cos(q_1),\, p_5\cos(q_2)\right]^T$,

$$M(q) = \begin{bmatrix} p_1 & p_3\cos(q_1-q_2)\\ p_3\cos(q_1-q_2) & p_2\end{bmatrix},$$

$$C(q,\dot{q}) = \begin{bmatrix} 0 & p_3\sin(q_1-q_2)\dot{q}_2\\ -p_3\sin(q_1-q_2)\dot{q}_1 & 0\end{bmatrix}.$$

The physical parameters which have been used for the numerical study (see Table I) are combined to

$$\begin{aligned}
p_1 &= l_1^2 m_2 + l_1^2 m_b + l_{1c}^2 m_1 + I_1\\
p_2 &= m_2 l_{2c}^2 + m_b l_2^2 + I_2\\
p_3 &= m_2 l_1 l_{2c} + m_b l_1 l_2\\
p_4 &= m_1 g l_{1c} + m_2 g l_1 + m_b g l_1\\
p_5 &= m_2 g l_{2c} + m_b g l_2\,.
\end{aligned}$$

TABLE I

PHYSICAL PARAMETERS OF THE PENDUBOT WITH SPRING-ARTICULATED ELBOW JOINT.

Parameter	First Link	Second Link	Ball
Length (m)	$l_1 = 0.4$	$l_2 = 0.48$	—
Mass (kg)	$m_1 = 2$	$m_2 = 1.8$	$m_b = 0.1$
Distance to CoM (m)	$l_{1c} = 0.2$	$l_{2c} = 0.24$	—
Inertia about CoM ($\mathrm{kg\,m^2}$)	$I_1 = m_1 l_1^2/12$	$I_2 = m_2 l_2^2/12$	—
Gravitational constant	$g = 9.81\,\mathrm{m/s^2}$		
Spring constant	$K = 6\,\mathrm{Nm/rad}$		
Spring offset	$q_{\mathrm{off}} = 0$		

TABLE II

SCALAR COEFFICIENT FUNCTIONS OF THE REDUCED DYNAMICS (8).

$$\begin{aligned}
\alpha \;=\;& \Bigg\{p_3 \cos\left(\phi(X_b) - \arccos\left(\frac{X_b - l_1\cos(\phi(X_b))}{l_2}\right)\right) \\
&- \frac{p_2\, l_1\, \sin(\phi(X_b))}{\sqrt{l_2^2 - [X_b - l_1\cos(\phi(X_b))]^2}}\Bigg\}\phi'(X_b) - \frac{p_2}{\sqrt{l_2^2 - [X_b - l_1\cos(\phi(X_b))]^2}} \\
\beta \;=\;& \Bigg\{p_3 \cos\left(\phi(X_b) - \arccos\left(\frac{X_b - l_1\cos(\phi(X_b))}{l_2}\right)\right) - \frac{p_2\, l_1\, \sin(\phi(X_b))}{\sqrt{l_2^2 - [X_b - l_1\cos(\phi(X_b))]^2}}\Bigg\}\left[\phi''(X_b)\right] \\
&- \Bigg\{\frac{p_2\left(l_1\cos(\phi(X_b)) + \frac{[X_b - l_1\cos(\phi(x_b))]\, l_1^2 \sin^2(\phi(X_b))}{l_2^2 - [X_b - l_1\cos(\phi(X_b))]^2}\right)}{\sqrt{l_2^2 - [X_b - l_1\cos(\phi(X_b))]^2}} \\
&\quad + p_3 \sin\left(\phi(X_b) - \arccos\left(\frac{X_b - l_1\cos(\phi(X_b))}{L_2}\right)\right)\Bigg\}\left[\phi'(x_b)\right]^2 \\
&- \frac{2\, p_2 [X_b - l_1\cos(\phi(x_b))]\, l_1 \sin(\phi(x_b))}{\sqrt[3]{l_2^2 - [X_b - l_1\cos(\phi(X_b))]^2}}\left[\phi'(X_b)\right] - \frac{p_2 [X_b - l_1\cos(\phi(x_b))]}{\sqrt[3]{l_2^2 - [X_b - l_1\cos(\phi(X_b))]^2}} \\
\gamma \;=\;& p_5 \frac{X_b - l_1\cos(\phi(X_b))}{l_2} + K\left(\arccos\left(\frac{X_b - l_1\cos(\phi(X_b))}{l_2}\right) - \phi(X_b) - q_{\mathrm{off}}\right)
\end{aligned}$$

TABLE III

REWRITING THE PERFORMANCE INDEX (11) INDEPENDENT OF $\phi''(\cdot)$.

$$\begin{aligned}
\exp\left\{2\int_{X_b(R)}^{s} \frac{\beta\left(\tau,\phi(\tau),\phi'(\tau),\phi''(\tau)\right)}{\alpha\left(\tau,\phi(\tau),\phi'(\tau)\right)} d\tau\right\} &= \exp\left\{2\int_{X_b(R)}^{s} \frac{\rho_1(\tau,\phi(\tau))\cdot\phi''(\tau) + \rho_3\left(\tau,\phi(\tau),\phi'(\tau)\right)}{\rho_1(\tau,\phi(\tau))\cdot\phi'(\tau) + \rho_2(\tau,\phi(\tau))} d\tau\right\} \\
&= \exp\left\{2\int_{X_b(R)}^{s} \frac{\left[\rho_1(\tau,\phi(\tau))\phi'(\tau) + \rho_2(\tau,\phi(\tau))\right]' - \rho_1'(\cdot)\phi'(\tau) - \rho_2'(\cdot) + \rho_3(\cdot)}{\rho_1(\tau,\phi(\tau))\phi'(\tau) + \rho_2(\tau,\phi(\tau))} d\tau\right\} \\
&= \exp\left\{2\int_{X_b(R)}^{s} \frac{\rho_3\left(\tau,\phi(\tau),\phi'(\tau)\right) - \rho_1'(\tau,\phi(\tau))\phi'(\tau) - \rho_2'(\tau,\phi(\tau))}{\rho_1(\tau,\phi(\tau))\phi'(\tau) + \rho_2(\tau,\phi(\tau))} d\tau\right\} \\
&\quad \times \left[\frac{\rho_1\left(s,\phi(s)\right)\cdot\phi'(s) + \rho_2\left(s,\phi(s)\right)}{\rho_1\left(X_b(0),\phi(X_b(0))\right)\cdot\phi'(X_b(0)) + \rho_2\left(X_b(0),\phi(X_b(0))\right)}\right]^2
\end{aligned}$$

B. Coefficients of the Reduced Dynamics

The scalar coefficient functions of (8) are listed in Table II.

C. Rewriting the Performance Index Independent of $\phi''(\cdot)$

We can rewrite the first factor of the performance index (11) independent of $\phi''(\cdot)$ as shown in Table III.

REFERENCES

[1] R. Alexander, "Three uses for springs in legged locomotion," *The International Journal of Robotics Research*, vol. 9, no. 2, pp. 53–61, 1990.

[2] V. Arnold, *Mathematical Methods of Classical Mechanics (Graduate Texts in Mathematics)*, 2nd ed. New York: Springer, 1989.

[3] S. Ichinose, S. Katsumata, S. Nakaura, and M. Sampei, "Throwing motion control experiment utilizing 2-link arm passive joint," in *Proc. 2008 SICE Annual Conference*, Tokyo, Japan, Aug. 2008, pp. 3256–3261.

[4] S. Katsumata, S. Ichinose, S. Nakaura, and M. Sampei, "Throwing motion control based on output zeroing utilizing 2-link underactuated arm," in *Proc. 2009 American Control Conference*, St. Louis, Missouri, USA, June 2009.

[5] A. Shiriaev, J. Perram, A. Robertsson, and A. Sandberg, "Periodic motion planning for virtually constrained Euler–Lagrange systems," *Systems and Control Letters*, vol. 55, pp. 900–907, 2006.

[6] T. Shoji, S. Nakaura, and M. Sampei, "Dexterous throwing motion control for an underactuated arm based on the analysis of zero dynamics," in *Proc. ICROS-SICE International Joint Conference 2009*, Fukuoka, Japan, Aug. 2009.

[7] M. Spong and D. Block, *Pendubot user manual*, University of Illinois, Urbana-Champaign, USA, 1996.

[8] C. Zone, "Baseball pitching robot," Patent 3 009 451, Nov., 1961. [Online]. Available: http://www.freepatentsonline.com/3009451.html